

2021

Development of a shoeboxing approach for Urban Building Energy Modeling

Federico Battini

Free University of Bozen-Bolzano, Italy, federico.battini@natec.unibz.it

Giovanni Pernigotto

Andrea Gasparella

Follow this and additional works at: <https://docs.lib.purdue.edu/ihpbc>

Battini, Federico; Pernigotto, Giovanni; and Gasparella, Andrea, "Development of a shoeboxing approach for Urban Building Energy Modeling" (2021). *International High Performance Buildings Conference*. Paper 385.

<https://docs.lib.purdue.edu/ihpbc/385>

This document has been made available through Purdue e-Pubs, a service of the Purdue University Libraries. Please contact epubs@purdue.edu for additional information. Complete proceedings may be acquired in print and on CD-ROM directly from the Ray W. Herrick Laboratories at <https://engineering.purdue.edu/Herrick/Events/orderlit.html>

Development of a shoeboxing approach for Urban Building Energy Modeling

Federico BATTINI^{1*}, Giovanni PERNIGOTTO², Andrea GASPARELLA³

¹Free University of Bozen-Bolzano, Faculty of Science and Technology,
Bolzano, Italy

Tel: +39 0471 017888, Fax: +39 0471 017009, email: federico.battini@natec.unibz.it

²Free University of Bozen-Bolzano, Faculty of Science and Technology,
Bolzano, Italy

Tel: +39 0471 017632, Fax: +39 0471 017009, email: giovanni.pernigotto@unibz.it

³Free University of Bozen-Bolzano, Faculty of Science and Technology,
Bolzano, Italy

Tel: +39 0471 017200, Fax: +39 0471 017009, email: andrea.gasparella@unibz.it

* Corresponding Author

ABSTRACT

Urban Building Energy Modeling aims at assessing the building energy performance at city scale with as little computational effort as possible. Thus, different methods have been developed in the last years to reduce the required calculation time by simplifying the modeling approach, selecting only representative buildings, or minimizing the building description. Starting from the latter ones, this work proposes a novel algorithm capable of abstracting a randomly shaped building into a representative shoebox. The presented shoebox generation algorithm is based on a preliminary sensitivity screening analysis on a set of reference parallelepiped-shaped thermal zones. This allowed the identification of the most significant geometry indicators influencing the building's performance. Based on this, more complex geometries have been simplified to the shoebox with the same indicators and the accuracy of the algorithm has been evaluated comparing the simulated performance of simplified and original buildings. The approach includes the definition of equivalent shading surfaces, to account for self-shading elements in the original building geometry. The algorithm has shown good accuracy not only on the hourly thermal loads, but also the zones' hourly temperature profiles, reducing to one third the energy simulation time with respect to the detailed building model. Although not as fast as other urban modelling approaches in the literature, it can retain accurate results at a finer time scale, i.e., on hourly basis, which is necessary in applications such as district heating and energy networks.

1. INTRODUCTION

Cities account for 60 to 80 % of the world's energy consumption and generate as much as 70 % of human-induced greenhouse gas emissions (United Nations Habitat, 2019). The building sector, in particular, is responsible for a large share of the overall energy use, corresponding for instance to 40 % in the European Union (European Parliament and Council of the European Union, 2010). Consequently, decreasing buildings' energy demand is essential to tackle the climate crisis. In the European Union, the current annual renovation rate of the building stock varies between 0.4 and 1.2 %, depending on the Member State, and it is largely insufficient for a fast reduction of the global building energy demand. By means of the European Green Deal, the European Commission aims at least to double the current renovation rate to meet its long-term climate objectives (European Commission, 2019). To achieve these goals, however, it is necessary to adopt new approaches in order to estimate the building energy demand at large spatial scales, focusing on groups of buildings and districts. Among the available alternatives, the most known is the Urban Building Energy Modeling *UBEM*, which allows for a bottom-up city-scale energy modeling using dedicated Building Performance Simulation codes (Johari *et al.*, 2020) specifically introduced to overcome the limitations of traditional

energy modeling at single building level. Indeed, the same workflow employed for characterizing the energy performance of a single building cannot be directly applied to large groups, since it would require too much information and would be too computationally demanding (Reinhart and Davila, 2015). Therefore, to guarantee time and efficiency, *UBEM* relies on domain and model simplifications (Abbasabadi and Ashayeri, 2019), such as (i) reduction of building definition complexity, (ii) introduction of simplification algorithms, and (iii) simulation of representative buildings out of the entire building stock.

The first option pertains thermal model definition and simulation choice, which can considerably reduce the simulation time compared to detailed models. For instance, building energy balance can be solved as a steady state heat balance for each single thermal zone, including the surrounding context (Nouvel *et al.*, 2013) or not (Dall'O *et al.*, 2012). Furthermore, the number of thermal zones can be reduced as well, ranging from multi-zone (Mastrucci *et al.*, 2014) to single-zone models (Caputo *et al.*, 2013).

The second possibility regards the introduction of less resource intensive procedures. Such approaches are very different from one another and include, for example, low order thermal network models (Lauster *et al.*, 2014), abstracting and arbitrary building massing into a meaningful group of thermal shoebox models (Dogan and Reinhart, 2013), and reorganizing the building geometries with functional clustering and radiation analysis scaling (İşeri and Dino, 2020).

The third alternative goes beyond the usual archetype definition, often employed mainly for defining buildings' non-geometrical features. Representative buildings are found by means of a set of descriptive indicators to capture the energy-relevant features such as physical, operational and contextual characteristics. In this way, a more generic approach is developed for stock classification considering the dynamic nature of the urban context (Ghiassi *et al.*, 2017).

Despite all solutions listed above, the optimization of *UBEM* computational efficiency is still an open issue (Hong *et al.*, 2019). In this work, taking advantage of previous studies showing the potential of shoeboxes in urban simulation (Dogan and Reinhart, 2017), a new simplification algorithm is proposed. The algorithm is meant to simplify each building in the urban model into an equivalent representative shoebox, taking into account buildings' adjacencies and context obstructions. With respect to similar approaches in the literature, the outlined algorithm aims to improve the accuracy of energy demand prediction when dealing with complex building geometries, even at fine time scales such as hourly, while reducing the computational cost of the simulation.

2. METHODOLOGY

The workflow to develop a shoeboxing approach for *UBEM* consists of three parts: (a) identification and selection of geometry indicators for building simplification through sensitivity analysis, (b) shoeboxing algorithm development, and (c) extensive test of algorithm effectiveness.

2.1 Geometry indicators identification and selection

To simplify a randomly shaped building into a meaningful shoebox, the first step is to identify a set of geometry indicators properly describing a building. In this work, geometrical indices employed in the literature have been considered and selected through a multivariate sensitivity analysis performed on annual (1) heating needs, (2) cooling needs, (3) heating peak loads, and (4) cooling peak loads.

2.1.1 Indicators identification: Geometrical indicators can describe either the building's footprint or the entire massing. As regards the former one, the polygon shape indices used by SAGA-GIS have been considered (Conrad, 2020). Concerning the latter one, this study has adopted the same indices used by Kodors (2017) for geometric feature selection at the urban level and by Ghiassi and Mahdavi (2017) for multivariate cluster analysis in the development of a reductive bottom-up urban energy model. Finally, the shape factor has been also considered, given its influence on the final energy demand (Danielski *et al.*, 2012). As a whole, 13 indicators have been used and tested.

2.1.2 Indicators selection: To select the most relevant indices affecting the thermal demand, a sensitivity analysis has been performed on a parallelepiped-shaped thermal zone, with a fixed height and length and depth varied between 4 and 12 m according to a parametric plan, as in previous studies (Pernigotto *et al.*, 2014). A portion of each envelope surface has been modelled as adiabatic to simulate adjacencies to thermal zones at the same conditions. The adiabatic fraction of each surface has been changed independently and can vary between 0 and 1, i.e., each surface can be totally exposed to the external environment or completely adiabatic.

Table 1: Spearman's rank correlation coefficients color-coded in grey scale to highlight correlations' strength (the darker the cell, the stronger the correlation).

Geometry index	Heating		Cooling	
	Annual	Peak	Annual	Peak
Plan area	0.43	0.55	0.18	0.37
Plan perimeter	0.43	0.55	0.18	0.37
Edge ratio	-0.43	-0.54	-0.18	-0.37
Elongation1	-0.10	-0.13	-0.05	-0.09
Elongation2	0.10	0.13	0.05	0.09
Eccentricity	-0.10	-0.13	-0.05	-0.09
Form factor	0.10	0.13	0.05	0.09
Compactness	-0.10	-0.13	-0.05	-0.09
Volume	0.43	0.55	0.18	0.37
Surface area	0.43	0.55	0.18	0.37
Shape factor	-0.43	-0.54	-0.18	-0.37
Non-adiabatic surface area	0.44	0.52	0.13	0.34
Non-adiabatic area shape factor	0.00	-0.04	-0.07	-0.04

Windows have been modelled as portions of the externally exposed vertical walls by a window-to-wall ratio ranging between 0 and 0.9. The geometrical definition of the model has been completed by adding vertical and horizontal overhangs whose depth can vary between 0 and 2.8 m. The opaque envelope has been characterized by an insulating and a massive layer, for which only the thickness has been considered as variable. The same wall composition, characterized by a thermal transmittance varying between 0.17 and 3.28 W m⁻² K⁻¹, has been applied to all opaque surfaces. Windows have been defined by means of the type of glass, filling gas and number of gaps, giving a total of 17 combinations with transmittance and solar heat gain coefficient ranging from 0.41 W m⁻² K⁻¹ and 0.49 to 5.75 W m⁻² K⁻¹ and 0.84, respectively. For the remaining heat balance contributions and boundary conditions time-constant values have been assigned. The ventilation rate has been expressed as air changes per hour ranging between 0 and 1. Internal gains varying from 0 to 8 W m⁻² have been included. Finally, the HVAC system has been considered as always active. Moreover, constant heating and cooling setpoints have been varied between 18 and 22 °C and from 22 to 30 °C, respectively.

As sampling technique, the Latin hypercube sampling has been used, and the number of variants has been progressively increased until convergence of the employed statistics has been reached. An overall number of 20000 different thermal zone configurations have been simulated with EnergyPlus, assuming ideal heating and cooling systems in the climate of Denver, Colorado. The Spearman's rank correlation coefficient ρ has been adopted. This statistic evaluates how well the relationship between two variables can be described by a monotonic function. It can be either positive or negative, i.e., $-1 \leq \rho \leq 1$. A value of $|\rho|$ larger than 0.7 points out a strong correlation, a value between 0.3 and 0.7 a moderate correlation, while a value lower than 0.3 a weak or even null correlation. ρ for each of the four simulation outputs has been computed for every investigated indicator. The outcome of the sensitivity analysis is reported in Table 1. Since a shoebox can be defined by three dimensions, it has been decided to select three indicators, in order to solve a system of three equations with three unknowns. Indicators have been selected considering the correlation strength, as well as their linear correlations. Furthermore, more complex indicators have been preferred to the simplest ones (e.g., although characterized by similar ρ , the edge ratio has been selected instead of area and perimeter). As shown in Table 1 and Equation (1), the selected indices are edge ratio, shape factor and the first elongation definition:

$$\begin{aligned}
 \text{edge ratio} &= \frac{\text{perimeter}}{\text{area}} \\
 \text{elongation} &= \frac{\text{minor length}}{\text{major length}} \\
 \text{shape factor} &= \frac{\text{surface area}}{\text{volume}}
 \end{aligned} \tag{1}$$

2.2 Shoeboxing algorithm development

Once the most meaningful indicators have been selected, it has been possible to proceed with the development of the simplification algorithm. The algorithm has been generated in the framework of Rhinoceros as CAD modeling platform, its plug-in Grasshopper, and EnergyPlus as Building Performance Simulation tool. In details, the workflow has been built in Grasshopper by means of customized components written in Python programming language. Geometrical modelling tasks have been implemented using RhinoCommon API (Robert McNell & Associates, 2020), while the conversion from massing model to thermal zones performed by using the Ladybug Tools core SDK (Ladybug Tools LLC, 2020). First, each building has been converted into a representative shoebox; then, the three selected indicators have been computed, based on its geometrical characteristics. The calculated indicators have been employed to estimate the representative shoebox's dimensions (x, y and z, respectively for width, depth and height) by solving a system of non-linear equations, as reported in Equation (2).

$$\left\{ \begin{array}{l} \text{edge ratio} = \frac{2(x+y)}{x \cdot y} \\ \text{elongation} = \frac{x}{y} \\ \text{shape factor} = \frac{2(x \cdot z) + 2(y \cdot z) + 2(x \cdot y)}{x \cdot y \cdot z} \end{array} \right. \quad (2)$$

The resulting shoebox has been characterized by the same window-to-wall ratio as the starting building and the same floor height. Also, the thermophysical properties have been assigned accordingly and the building's self-shading included. Specifically, the impact of the building's self-shading has been taken into account through equivalent shading surfaces obstructing a portion of the windows. Those shading elements have been determined by means of a radiation analysis performed on both starting geometry and resulting shoebox according to the all-weather Perez sky model. For sake of simplicity, for the starting geometry the radiation analysis focused only on the windows' areas, while the entire geometry has been accounted for in the shoebox. Since considering only windows surfaces has considerably reduced the area to analyse, a calculation grid of 0.2 m has been employed. The average annual entering radiation has been obtained for each cardinal direction and floor for both models, and the ratios between starting geometry and shoebox results computed. Then, an equivalent obstruction ratio has been calculated for each façade and floor:

$$\text{obstruction ratio} = 1 - \frac{\text{starting geometry entering radiation}}{\text{shoebox entering radiation}} \quad (3)$$

For every window in a given floor and façade of the simplified shoebox model, the corresponding ratio has been used to calculate the equivalent shading area out of the window's area. The modelled shadings have the same height of the window, while their length has been computed to match the equivalent shading area calculated before. The equivalent shading surfaces have been placed 1 cm outside the window to fully obstruct all incident radiation. In this research, the starting building and the corresponding shoebox have been modelled as stand-alone since the focus has been put on the determination of equivalent shading surfaces to account for self-shading. Nevertheless, this approach can be generalized to account for the urban context by modelling also the building's surroundings. Moreover, also adjacencies can be taken into account by means of adiabatic elements in the facades, whose ratios can be computed independently for each cardinal direction by analyzing the façades of the starting building and considering a $\pm 45^\circ$ tolerance range. As a final step, detailed and simplified models have been automatically exported as idf files and edited by means of Python scripts with the aid of the library eppy (Philip, 2020), to interface EnergyPlus with Python language.

2.3 Extensive test

The driving purpose of the proposed algorithm is the improvement in building's performance prediction when dealing with complex massing shapes. In the literature, various works studying the urban context relied on the creation from scratch of sample neighborhoods (Lyu *et al.*, 2019), urban layouts (Xu *et al.*, 2019) or building grid models (Natanian *et al.*, 2019). However, in such configurations buildings are simple in shape, mainly with rectangular footprints. Furthermore, the same pattern is repeated to parametrically generate buildings' arrangement.

Table 2: Number of polyominoes depending on the number of cells

Number of cells	1	2	3	4	5	6	7	8	9	10
Number of polyominoes	1	1	2	5	12	35	108	369	1285	4655
Polyominoes with holes	0	0	0	0	0	0	1	6	37	195
Polyominoes without holes	1	1	2	5	12	35	197	363	1248	4460

Differently, Javanroodi *et al.* (2018) employed a series of form generation rules based on a basic module to generate buildings' forms based on urban density ranges. In this work a similar approach has been adopted, defining buildings' shapes out of polyominoes (Golomb, 1994) in order to guarantee complex and various shapes. A polyomino is created out of square cells by joining one or more squares edge to edge; their number increases according to the number of cells following the integer sequence A000105 (Sloane, 2020), as reported in Table 2. To keep the size of the analysis manageable, the number of cells utilized to create polyominoes has been varied between two and six. Among them, rectangular in shape geometries have been discarded, resulting in 48 unused forms. Figure 1(a) reports all possible 55 shapes, which have been used as base for the building geometries. As reported in Table 2, up to six cells no polyomino has holes. Therefore, courtyard buildings are not considered in this analysis unlike other studies (Javanroodi *et al.*, 2019). Nevertheless, the variety of shapes considered, even without courtyard, has been considered adequate to guarantee properly testing of the algorithm. To be consistent with the sensitivity analysis previously performed, polyominoes have been generated from a starting square cell with an edge of 4 m. To explore the space of solutions as much as possible, each resulting shape has been: (i) rotated according to the four cardinal points, (ii) scaled by a factor equal to one, two, three or four, and (iii) extruded by a number of floors equal to one, two, three or four, with each floor 3 m tall. Thus, from each polyomino, a total of 58 building shapes has been generated, as shown for instance in Figure 1(b). The total amount of generated buildings to be simulated has been 3072.

Once all building shapes have been generated, each building has been converted into its representative shoebox according to the simplification algorithm. At this point, the same thermophysical and operational features have been assigned to every simulation file (Table 3). The envelope definition is the same for every external opaque surface, with an external insulating and an internal massive layer, i.e., polystyrene and concrete respectively. As for the envelope, one definition has been adopted for the windows as well. For sake of simplicity, the frame has been neglected and a triple glass window with air filling (3 mm clear glass panels, with the innermost panel with low-e treatment, and 6 mm air gaps) has been considered. Finally, to test the effectiveness of the algorithm under different boundary conditions, the buildings have been simulated in three climates - Bolzano and Messina, Italy, and Denver, U.S., selected to include both a heating- (Bolzano) and a cooling-dominated (Messina) climate, as well as a climate characterized by large daily temperature variations (Denver).

The investigated outcomes of this research have been both temperature and energy needs. The temperature output has been evaluated on hourly basis, considering just the hours for which the temperature is larger than 20 °C and lower than 26 °C, and calculating also the annual positive and negative maximum differences. To understand how well the simplification algorithm performs overall, the share of hours in which the hourly deviation lays within ± 0.5 °C has been calculated. The energy needs have been analyzed at annual and hourly scale. Annual absolute and relative differences between detailed and simplified models have been computed and the Root Mean Square Error *RMSE* calculated. Furthermore, the percentage of hours of the entire year in which the hourly difference between the models lays within specific intervals (i.e., ± 5 %, ± 10 %, ± 20 %) has been computed to assess hourly deviations. Such evaluations have been carried out at building and floor level, since every floor has been modelled as a thermal zone.

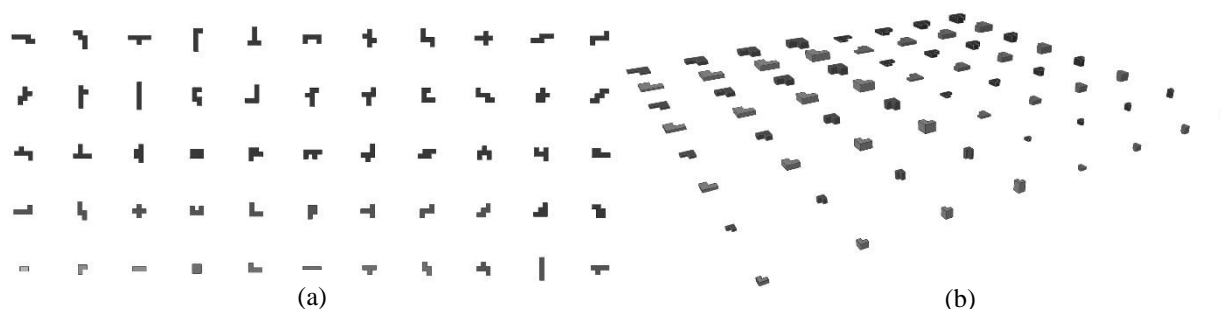


Figure 1: (a) Possible polyominoes obtained by combining up to 6 square cells and (b) all buildings' combinations resulting from one polyomino's footprint after rotation, scaling and extrusion

Table 3: Energy model settings

OPAQUE ENVELOPE					
Layer	Thickness [m]	Thermal conductivity [$\text{W m}^{-1} \text{K}^{-1}$]	Specific heat capacity [$\text{J kg}^{-1} \text{K}^{-1}$]	Density [kg m^{-3}]	U-Value no film [$\text{W m}^{-2} \text{K}^{-1}$]
Polystyrene	0.1	0.05	1470	40	0.329
Concrete	0.2	0.37	840	1190	
FENESTRATION					
Window-to-wall ratio	Glass U-Value [$\text{W m}^{-2} \text{K}^{-1}$]		Glass SHGC	Glass Visible Transmittance	
40 %	1.772		0.578	0.698	
HEATING SYSTEM			COOLING SYSTEM		
Setpoint	Schedule	Type	Setpoint	Schedule	Type
20 °C	Always ON	Ideal	26 °C	Always ON	Ideal
VENTILATION			INTERNAL GAINS		
Type	Rate [ach]	Schedule	Type	Power [W m^{-1}]	Schedule
Infiltration	0.3	Always ON	Other equipment	0.3	Always ON

3. RESULTS AND DISCUSSION

3.1 Overview

Temperature and energy needs differences between the detailed and simplified models are presented by means of boxplots and histograms. Regardless the magnitude of the deviation occurring, the shoeboxing algorithm reduced the time required for the thermal simulation to one third for the simplified models with respect to the detailed ones for all the considered cases.

3.2 Temperature

Figure 2 reports the boxplots regarding the share of hours for which the temperature deviation in each floor lays within ± 0.5 °C for the three climates. Bolzano and Messina show a similar behavior: for both climates the temperature deviations lay within ± 0.5 °C for more than 95 % of time for all simulated floors, excluding the outliers, and the temperature prediction for Bolzano is the most accurate overall. On the contrary, the outputs obtained for Denver are less accurate: indeed, excluding the outliers, temperature deviations stay within the ± 0.5 °C interval for only at least 75 % of time, depending on the considered floor.

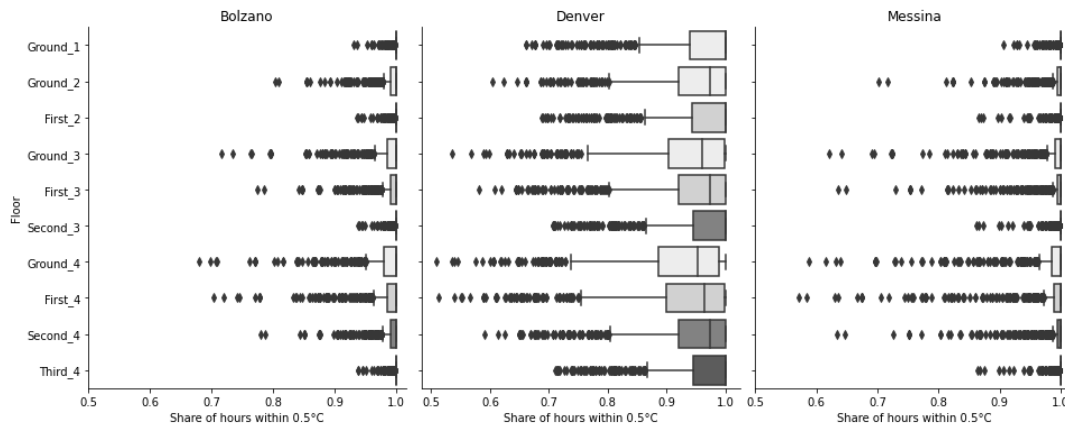


Figure 2: Resulting boxplots of the share of hours within ± 0.5 °C temperature deviation for each floor. Outliers are plotted outside the boxes' whiskers. The floors, color-coded in grey scale, are indicated with the floor name and the number of floors present in the building of which the floor is part of.

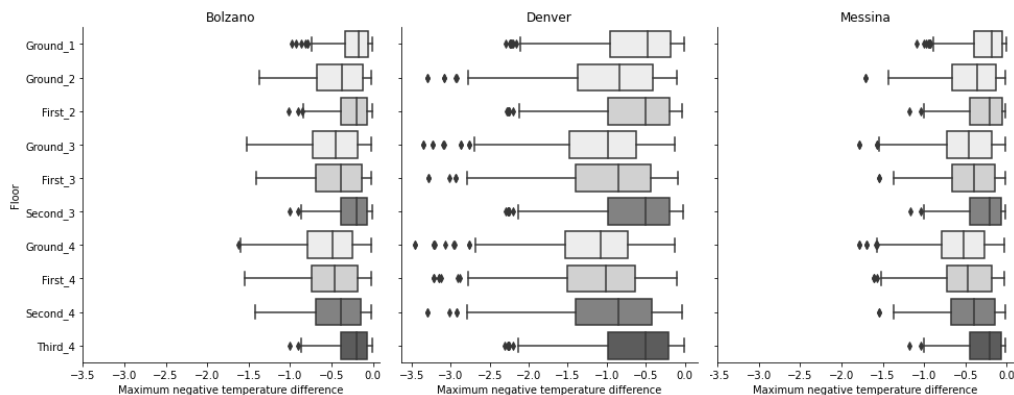


Figure 3: Resulting boxplots of the largest negative temperature difference

The most shaded floors are characterized by the largest temperature deviations. This has been observed in all the considered climates and particularly in Denver. Moreover, the higher the number of floors, the lower the accuracy. Finally, the maximum positive and negative temperature deviations are often included within the ± 0.5 °C interval for the climates of Bolzano and Messina, while larger differences occur for the climate of Denver. Such behaviour is shown by Figure 3 in which the boxplot regarding the largest negative temperature differences are reported. The largest positive temperature differences, even though not reported, experience lower differences.

3.3 Heating and cooling needs

The energy need has been investigated on annual and hourly basis. Figure 4 and Figure 5 depict with boxplots the relative differences of heating and cooling needs, as well as the *RMSEs*. As for the temperatures, it is possible to see that the climate of Bolzano is the one with the best predictions: indeed, the heating need stays within ± 5 % for all buildings and the cooling need within ± 10 % for the most of them. The accuracy of this prediction is confirmed also by the *RMSE* values. The climate of Messina may seem the one with the worst predictions, in particular regarding the heating need. However, from Figure 6 it is clear that the large relative deviations are mainly due to the very low magnitude of the heating needs. As it can be noticed in Figure 6 and Figure 7, the results obtained in the climate of Denver are overall the least accurate. Nonetheless, Figure 4 shows that the model annual need predictions do not exceed ± 10 % and ± 20 % deviation, respectively for cooling and heating and for most of buildings. Figure 6 and Figure 7 also highlight how, for the considered climates, the heating demand is underestimated when not properly predicted. On the contrary, the cooling demand is generally overestimated by the simplified model. This behavior can be explained considering that the simplified shoeboxes are smaller than the starting geometry. Even if the obstruction is properly shading the windows and the solar heat flux entering in the zone is the same for both models, since the volume of air is lower in the simplified model, so is its capacitance – consequently, a slightly different impact of solar gains is obtained. Overall, it is possible to see that the deviations increase with the number of floors, as a consequence of larger deviations occurring at the lower floors as observed also in the analysis of temperature deviations.

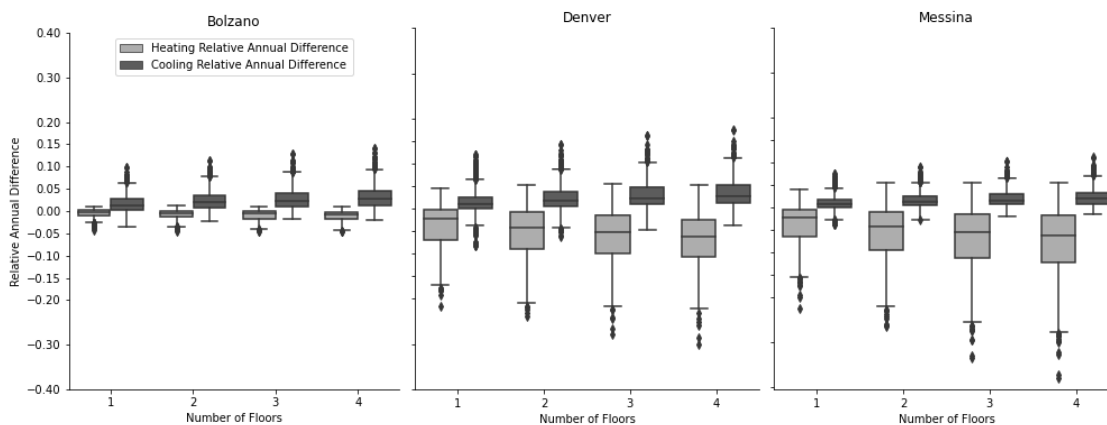


Figure 4: Boxplots for annual heating and cooling needs relative differences in function of buildings' number of floors

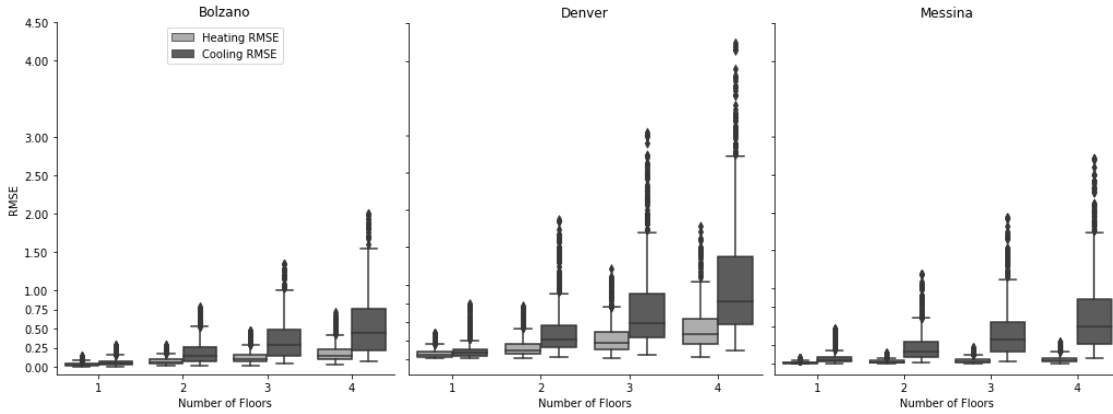


Figure 5: Boxplots for annual heating and cooling *RMSE* in function of buildings' number of floors

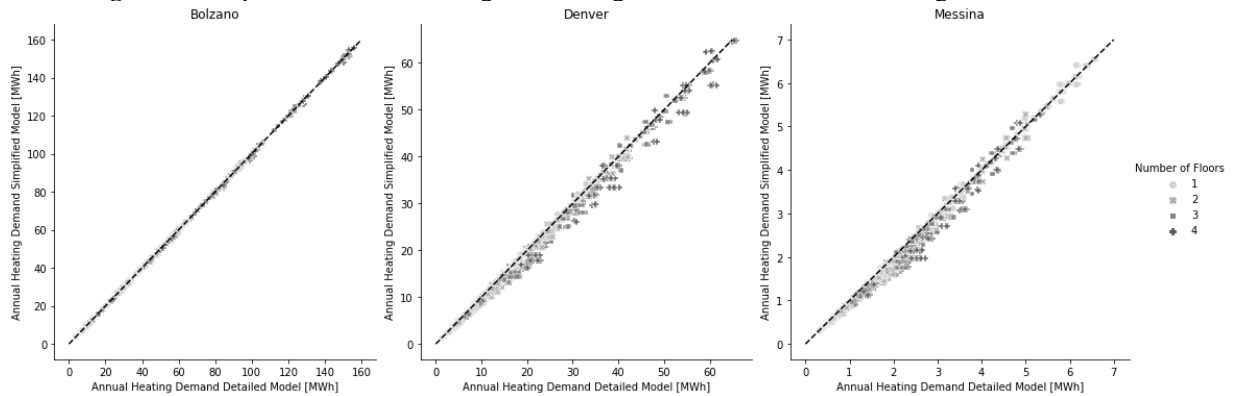


Figure 6: Simplified and detailed model heating annual outcomes in function of buildings' number of floors

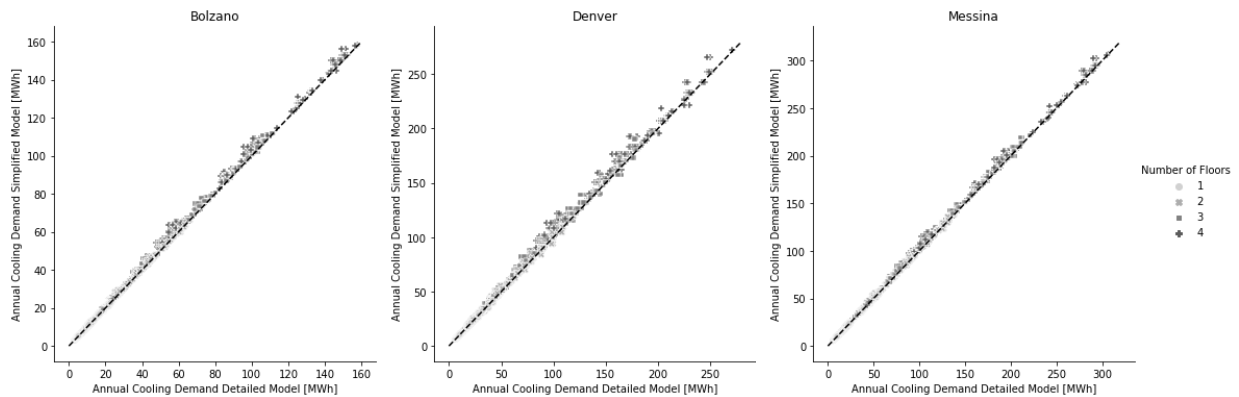


Figure 7: Simplified and detailed model cooling annual outcomes in function of buildings' number of floors

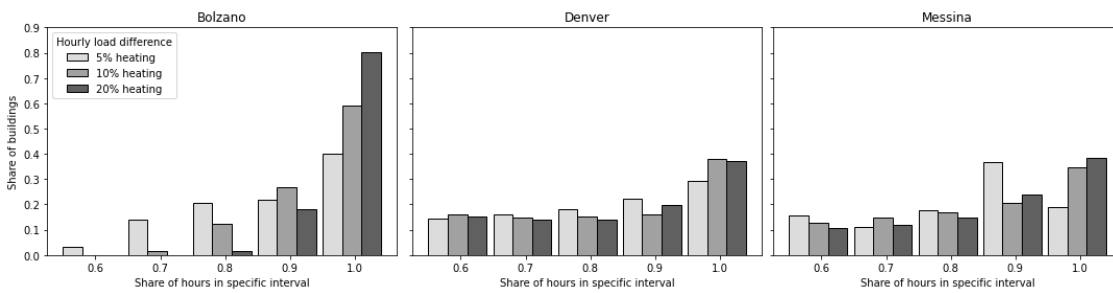


Figure 8: Share of buildings within a specific hourly heating range for a certain number of hours along the year

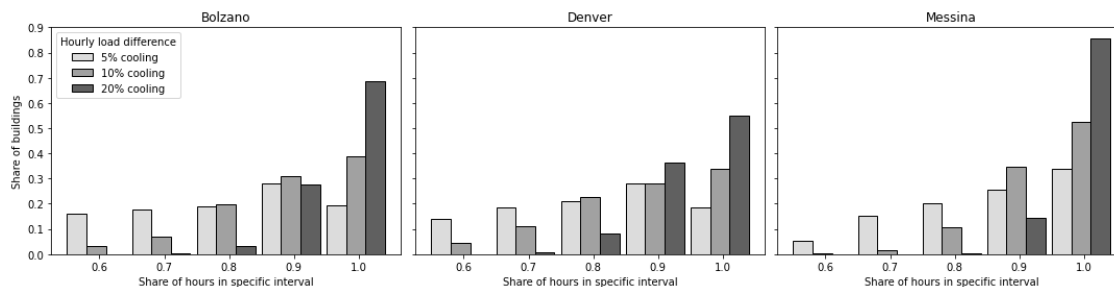


Figure 9: Share of buildings within a specific hourly cooling range for a certain number of hours along the year

Regarding the hourly energy needs, Figure 8 and Figure 9 report the share of buildings for which the relative hourly deviations lay within three deviation intervals (5 %, 10 % and 20 %) for a certain time of the year.

As for the annual needs, the outputs of Bolzano are those with the best prediction for the heating: up to 70 % of buildings have more than 90 % of hours along the year with a maximum relative deviation between the detailed and simplified model of ± 20 %. Furthermore, all buildings are in this interval if the minimum percentage of hours considered is 70 %. Regarding the cooling needs, hourly accuracy is lower. The hourly results for the climates of Denver and Messina are aligned to the annual ones. Messina shows lower accuracy for the heating demand, but, as seen for the annual results, it is related to the very low magnitude of the needs. Instead, the cooling hourly prediction is the best among the three cases. Denver shows higher accuracy in cooling estimation with respect to heating. This is not only due to the capability of the algorithm but also to the lower magnitude of the heating needs with respect to the cooling ones.

Although floor level results have not been reported, they show the same behavior of the building level outcomes and they underline how the prediction for the least shaded floors is the most precise.

Finally, even though it seems that on the hourly basis the need prediction is less accurate, a closer look at the data reveals that larger deviations occur in hours characterized by lower energy needs. For what concerns the heating demand, peak loads and those periods of the year with higher demands are well predicted.

4. CONCLUSIONS

In this work, a novel simplification algorithm to ease *UBEM* computing resources has been presented. The algorithm aims at simplifying complex building shapes into representative shoeboxes, in order to reduce the required simulation time without compromising modeling accuracy and resolution. The automated simplification procedure creates the simplified model from a set of geometry indicators, includes equivalent shading surfaces to account for self-shading elements and defines a thermal zone for each of the building floors. To test the proposed approach, 3072 buildings have been generated and simplified into representative shoeboxes. Both detailed and simplified models have been simulated in three different climatic conditions, and hourly temperatures and heating and cooling needs analyzed. The algorithm has shown a good level of accuracy in estimating both hourly and annual needs, as well as temperature profiles for each floor, reducing the time required for the simulation to one third for the simplified models with respect to the detailed ones. However, larger discrepancies have been observed in climates characterized by quick temperature variations and large daily temperature differences.

In order to further improve the proposed algorithm, a thorough analysis of outliers will be performed in future developments, with the aim to optimize the shoebox definition and to increase the prediction accuracy. Moreover, the shoeboxing procedure efficacy will be also tested by considering the context and adjacent buildings, paving the way to the implementation in a urban model made of building shoebox metamodels, allowing to increase considerably the computational efficiency.

REFERENCES

- Aasabadi, N., & Ashayeri, M. (2019). Urban energy use modeling methods and tools: A review and an outlook. *Building and environment* 161.
- Caputo, P., Costa, G., & Ferrari, S. (2013). A supporting method for defining energy strategies in the building sector at urban scale. *Energy Policy*, 261-270.
- Conrad, O. (2020, August 6th). *Tool Polygon Shape Indices*. Retrieved from SAGA-GIS Tool Library Documentation (v7.1.1): http://www.saga-gis.org/saga_tool_doc/7.1.1/shapes_polygons_7.html

- Dall'O, G., Galante, A., & Torri, M. (2012). A methodology for the energy performance classification of residential building stock on an urban scale. *Energy and Buildings*, 211-219.
- Danielski, I., Fröling, M., & Joelsson, A. (2012). The Impact of the Shape Factor on Final Energy Demand in Residential Buildings in Nordic Climates. *WREF - The World Renewable Energy Forum*. Denver.
- Dogan, T., & Reinhart, C. (2013). Automated conversion of architectural massing models into thermal 'shoebox' models. *Proceedings of BS2013: 13th Conference of International Building Performance Simulation Association, Chambéry, France, August 26-28*, (pp. 3745-3752). Chambéry.
- Dogan, T., & Reinhart, C. (2017). Shoeboxer: An algorithm for abstracted rapid multi-zone building energy model generation and simulation. *Energy and Buildings*, 140, 140-153.
- European Commission. (2019, 12 11). The European Green Deal. Brussels.
- European Parliament and Council of the European Union. (2010, May 19). Directive 2010/31/EU of the European Parliament and of the Council on the energy performance of buildings. Official Journal of the European Union.
- Ghiassi, N., & Mahadavi, A. (2017). Reductive bottom-up urban energy computing supported by multivariate cluster analysis. *Energy and Buildings*, 372-386.
- Ghiassi, N., Tahmasebi, F., & Mahdavi, A. (2017). Harnessing buildings' operational diversity in a computational framework for high-resolution urban energy modeling. *Building Simulation*, 1005-1021.
- Golomb, S. W. (1994). *Polyominoes: Puzzles, Patterns, Problems, and Packings*. Princeton, New Jersey: Princeton University Press.
- Hong, T., Chen, Y., Luo, X., Luo, N., & Lee, S. (2019). Ten questions on urban building energy modeling. *Building and Environment*, 168.
- İşeri, O. K., & Dino, İ. G. (2020). An Algorithm for Efficient Urban Building Energy Modeling and Simulation. *2020 Proceedings of the Symposium on Simulation for Architecture and Urban Design*, (pp. 455-462).
- Javanroodi, K., Mahdavinejad, M., & Nik, V. M. (2018). Impacts of urban morphology on reducing cooling load and increasing ventilation potential in hot-arid climate. *Applied Energy*, 714-746.
- Javanroodi, K., Mahdavinejad, M., & Nik, V. M. (2019). A novel design-based optimization framework for enhancing the energy efficiency of high-rise office buildings in urban areas. *Sustainable Cities and Society*.
- Johari, F., Peronato, G., Sadeghian, P., Zhao, X., & Widén, J. (2020). Urban building energy modeling: State of the art and future prospects. *Renewable and Sustainable Energy Reviews*.
- Kodors, S. (2017). Geometric Feature Selection of Building Shape for Urban Classification. *Environment Technology Resources Proceedings of the International Scientific and Practical Conference*, (pp. 78-83). Rezekne.
- Ladybug Tools LLC. (2020, October 7). Retrieved from Ladybug Tools: www.ladybug.tools
- Lauster, M., Teichmann, J., Fuchs, M., Streblov, R., & Mueller, D. (2014). Low order thermal network models for dynamic simulations of buildings on city district scale. *Building and Environment*, 223-231.
- Lyu, T., Buccolieri, R., & Gao, Z. (2019). A Numerical Study on the Correlation between Sky View Factor and Summer Microclimate of Local Climate Zones. *Atmosphere*.
- Mastrucci, A., Baume, O., Stazi, F., Salvucci, S., & Leopold, U. (2014). A GIS-based approach to estimate energy savings and indoor thermal comfort for urban housing stock retrofitting. *BauSIM 2014*, (pp. 190-197). Aachen.
- Natanian, J., Aleksandrowicz, O., & Auer, T. (2019). A parametric approach to optimizing urban form, energy balance and environmental quality: The case of Mediterranean districts. *Applied Energy*.
- Nouvel, R., Schulte, C., Eicker, U., Pietruschka, D., & Coors, V. (2013). CityGML-based 3D city model for energy diagnostics and urban energy policy support. *Proceedings of BS2013: 13th Conference of International Building Performance Simulation Association, Chambéry, France, August 26-28*, (pp. 218-225). Chambéry.
- Pernigotto, G., Prada, A., Gasparella, A., & Hensen, J. (2014). Development Of Sets Of Simplified Building Models For Building Simulation. *International High Performance Buildings Conference*. Purdue.
- Philip, S. (2020). *scripting language for E+*, *Energyplus*. Retrieved from <https://github.com/santoshphilip/eppy/>
- Reinhart, C., & Davila, C. (2015, December 2). Urban building energy modeling - A review of a nascent field. *Building and Environment*, 97, 196-202.
- Robert McNell & Associates. (2020, August 6). *RhinoCommon API*. Retrieved from Rhino Developer Docs: https://developer.rhino3d.com/api/RhinoCommon/html/R_Project_RhinoCommon.htm
- Sloane, N. A. (2020). *A000105 Number of free polyominoes (or square animals) with n cells*. Retrieved from The online encyclopedia of integer sequences: <https://oeis.org/A000105>
- United Nations Habitat. (2019). The strategic plan 2020-2023.
- Xu, X., Liu, Y., Wang, W., Xu, N., Liu, K., & Yu, G. (2019). Urban Layout Optimization Based on Genetic Algorithm for Microclimate Performance in the Cold Region of China. *Applied sciences*.